Controlled reflectance surfaces with film-coupled colloidal nanoantennas : Supplementary Information

SUPPLEMENTARY FIGURE AND LEGEND

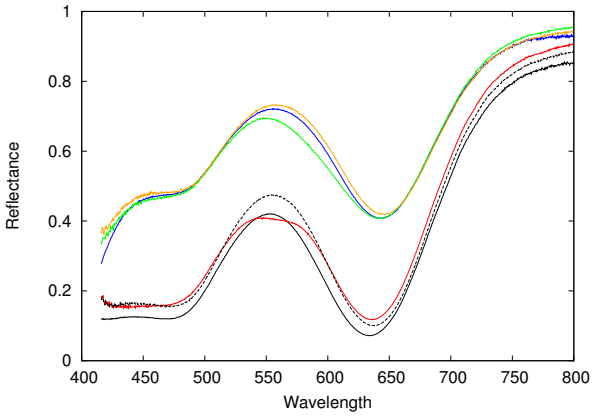

FIG. 1. Experimental reflectance normalized to the reflectance of a bare gold film for a 7.3% (upper curves) and a 17.1% (lower curves) concentrations for normal incidence (blue and black curves), for P polarization (green and red curves) and S polarization (orange and black dotted curves) at 25° incidence.These results show that the position of the resonance is not significantly sensitive to any of these parameters.

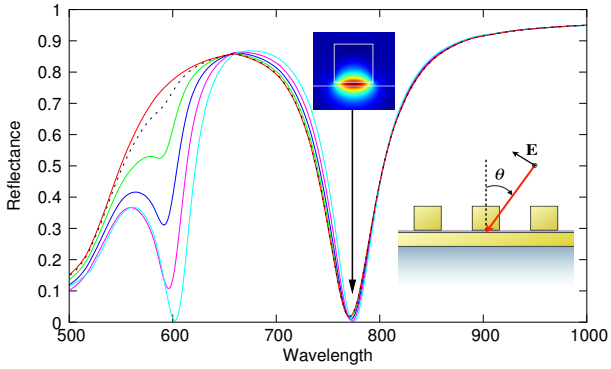

FIG. 2. Absorption resonances for the nanorods coupled to a gold film. Reflectance spectra of a periodic array of 74 nm wide gold rods, 4 nm above a gold film, for incidence angles ranging from 0° (red curve) to 25° (light blue curve) by 5° steps, in p-polarization (out-of-plane magnetic field). The fundamental resonance at 773 nm is insensitive to the incidence angle. The excitation of another resonance at 600 nm for non-normal incidence is a signature of an interferometric control of the absorption[11] arising from asymmetric excitation of the waveguide modes that exist in the metal-dielectric-metal region under the cube. The top inset shows the out-of plane magnetic field corresponding to the resonance.

SUPPLEMENTARY DISCUSSION

Physical behavior of the quasi-bidimensional structure

In this section, the physical behavior of the quasi-two-dimensional structure (gold nanorods on top of a gold film) is discussed in detail using Fourier Modal Method simulations. As has been underscored in prior work[8], the optical properties of the nanorods are very close to those of nanocubes, so that the more easily simulated nanorod system can be used to illustrate numerous aspects of the enhanced absorption by nanocubes, including the cavity behaviour of the gap, and the interferometic control of the absorption. Figure 2 shows a typical reflectance spectrum for gold nanorods on top of a gold film.

The fundamental mode in a perfect air- or dielectric-filled metallic waveguide is a mode that presents no cut-off - it is supported whatever the thickness of the waveguide and the frequency considered. A metal-dielectric-metal structure, with a perfect metal (all fields excluded), also supports this kind of fundamental mode. When the metal is not perfect, the effective index of the mode is larger than the index of the dielectric[16], so that the field is evanescent in the direction perpendicular to the interfaces. For this reason, the fundamental mode is very often referred to as a coupled plasmon mode - although this picture may not be the most appropriate - or as a gap-plasmon.

The effective index of the mode can be found by solving the dispersion relation

$$\kappa \tanh \frac{\kappa g}{2} + \frac{\kappa_m}{\epsilon_m} = 0 \qquad (1)$$

where g is the size of the gap, $\kappa = k_0 \sqrt{n_e^2 - 1}$ and $\kappa_m = k_0 \sqrt{n_e^2 - \epsilon_m}$, ϵ_m being the permittivity of the metal and $k_0 = \frac{2\pi}{\lambda_0}$ where λ_0 is the wavelength in the vacuum. This dispersion relation can be solved for complex values of n_e once the wavelength has been chosen: zeros of the left-hand part of the equation can be found using steepest-descent methods in the complex plane.In the case where the gap is 4 nm wide, at 773 nm, the complex effective index is $n_e = 4.34378 + 0.11961i$, showing that the gap-plasmon mode can propagate over more than 1 micron before suffering any significant losses. The corresponding effective wavelength of the mode is 177.8 nm.

Figure 3 shows the effective index as a function of the distance between the metallic interfaces.

In order to assess the nature of the resonance supported by the gaps under the rods, we vary the width of the rod (which represents the length of the cavity, w) keeping all the other geometrical parameters constant.

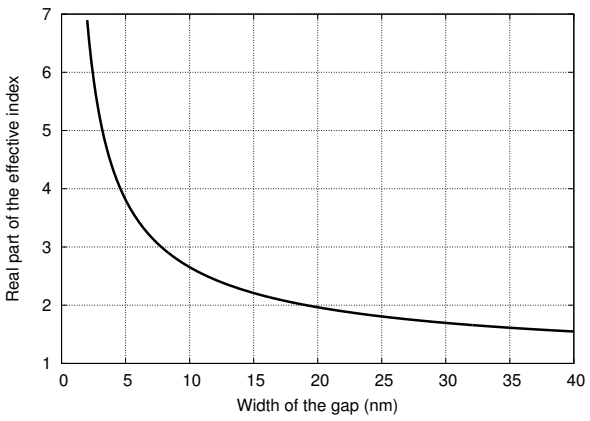

FIG. 3. Real part of the effective index of the guided mode inside the gap between two metallic walls as a function of the width of the gap.

The reflectance at normal incidence of the whole structure at $\lambda_0 = 773\,\text{nm}$ is shown in Fig. 4 as a function of the rod width. Minima in the reflectance are found to correspond to cavity resonances that possess an odd number of antinodes.

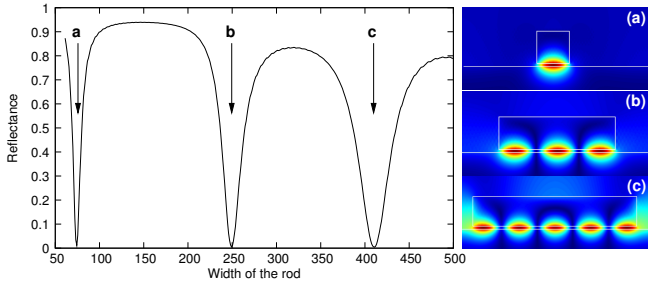

FIG. 4. Theoretical reflectance, at normal incidence and for p polarization, as a function of the rod's width, w. The distance between the first and the second peak corresponds precisely to the effective wavelength of the mode supported by the gap $\lambda_e = 177.8$ nm. The out-of-plane magnetic field is plotted for each resonance, showing the cavity modes with an odd number of antinodes.

Cavity resonances correspond to the build-up of a standing wave in the gap under the cube. When the nanocubes are excited by waves incident at normal incidence with respect to the surface, the cavity is excited uniformly on either side of the rod, so that the resonance can be seen as the interference between two counter propagating cavity modes: one excited from the left of the rod and one excited from the right. For an even number of antinodes, the interference is destructive, leading to a complete cancellation of the resonance. For an odd number of antinodes, the interference is constructive, leading to a doubling of the field amplitude in the cavity and a multiplication of the absorption by a factor of four. This is an exact example, in a nanometric device, of interferometric control of the absorption, as has been recently demonstrated[11].

We emphasize here that the first resonance appears for $w = 0.416\lambda_e$, smaller than the usual $\frac{\lambda_e}{2}$ limit associated, for example, with classical Fabry-Perot interferometers in optics or patch antennas in microwave technology. Such cavity resonances can occur when the condition

$$\arg(r) + \frac{2\,\pi\,w}{\lambda_e} = m\pi \tag{2}$$

is satisfied, where m is an integer and r is the reflection coefficient of the mode at the end of the gap. The reflection coefficient can easily be computed numerically. In plasmonic structures, such reflection coefficients may present phases that are very different from classical cases[19], leading here, with a phase for r of $-150°$ (and a reflection of 89.79%), to a further enhancement of the confinement.

Since the enhanced absorption is related to cavity resonances localized under the rod, the wavelength at which they are excited depends only on r and n_e. Since these two quantities do not change with the angle of incidence, the position of the resonance is expected to be insensitive to the incidence angle. Any change in the angle of incidence will however break the symmetry between the incident field coming from the right of the rod and the incident field coming from the left, lowering the impact of the interferometric control on the absorption. In particular, resonances presenting an even number of antinodes are not cancelled any more for non-normal incidence and another absorption peak that can be attributed to these resonances is observed in the reflectance (see Fig. 2).

Finally, when the size of the rods (the length of the cavity) is kept constant but the thickness of the gap changes, the variation of the wavelength λ_0 for which a resonance is excited satisfies

$$\lambda_0 = n_e\,\frac{2\pi\,w}{m\pi - \arg(r)}. \tag{3}$$

This means that the variation of λ_0 reproduces exactly the variation of the effective index (provided the phase of the reflection coefficient can be considered as constant, which is usually the case) explaining the somewhat universal shape of the curve giving the position of the resonance as a function of the spacer thickness - for cubes as well as for rods. This holds even when the waveguide is not symmetric (with silver on one side for instance).

The periodicity of the structure plays no role in the results that are presented above because the period is smaller than the wavelength. When this period is of the order of the wavelength, or when large incidence angle are considered, the grating constituted by the rods allows for the coupling of surface plasmons that couple to the resonances under the cube. This leads to a splitting and a shift of the cavity resonances, as shown Fig. 5. For all of our simulations employing periodic boundary

conditions, we have carefully checked that the scattering characteristics (especially the position of the resonance) do not depend on the periodicity. As the analysis above has very clearly shown, the resonance of interest for enhanced absorption can be correlated with a pure cavity resonance.

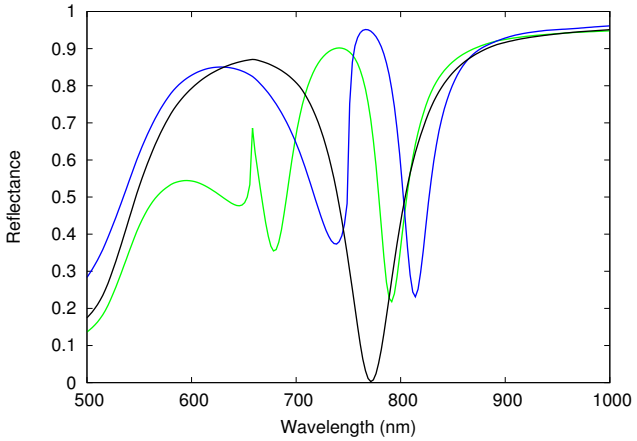

FIG. 5. Reflectance for three cases : when the periodicity (400 nm period) plays no role (black curve); when the period (750 nm) is of the order of the wavelength (blue curve); when the angle of incidence (45°, for a 500 nm period) is large (green curve).

Critical density

We derive here an approximate expression, valid for nanorods, for the critical period at which the electrical currents are balanced by magnetic ones. This expression be written as

$$d \simeq 4\, f\, g. \tag{4}$$

where d is the average spacing between nanorods (or periodicity, if the nanorods are distributed periodically). We begin by assuming that the metal is perfect, so that each cube can be treated as a perfect patch antenna. In that case, given the geometry of the problem, the field is essentially constant throughout any vertical section of the gap under the cube. For simplicity, let us assume a periodic system (even if the result can be generalized to any disordered structure) and take $z_0 = 1$. In the absence of nanocubes, the surface density of electrical currents on the surface of the metal due to the incident wave is given by

$$\mathbf{K}_E = \mathbf{H} \times \hat{n} \tag{5}$$

where $\hat{n}$ is the unitary vector normal to the surface. F For waves incident normal to the surface, $K_E = H_0 = E_0$ (for convenience, we take the wave impedance to be unitless, or $z_0 = 1$) where E_0 (resp. H_0) is the modulus of the incident electric (resp. magnetic) field. When the nanorods are introduced, they can be modeled as 2D patch antennas, with their edges considered as magnetic walls. We consider here that the nanorods are oriented such that the magnetic field lies along the width of the rods. Classical antenna theory suggests that the height of each magnetic wall is g, where g is the size of the gap – but that the effective height is $2g$ because the perfect metallic film acts as a mirror that doubles the effective height of the magnetic walls. Since there are two walls (and thus sources of magnetic currents) on each nanorod, the total area of magnetic current is $4g$ per unit length of rod.

Just as the electric surface currents are given by the modulus of the magnetic field at the surface of magnetic walls, the magnetic current density is given by the electric field. Its modulus can be written $E_f = f\, E_0$ where f is the enhancement of the field associated with the resonance of the optical patch antenna. Since $f >> 1$, it is possible to reach a high average magnetic current on the surface, even with a small surface coverage and a small ratio g/d. The average magnetic current density is then

$$K_M = \frac{f\, E_0\, 4\, g}{d}. \tag{6}$$

The critical density is reached when the condition $K_M \simeq K_E$ can be satisfied. In the present case, this directly leads to

$$d \simeq 4\, f\, g. \tag{7}$$

Size dispersion of the cubes

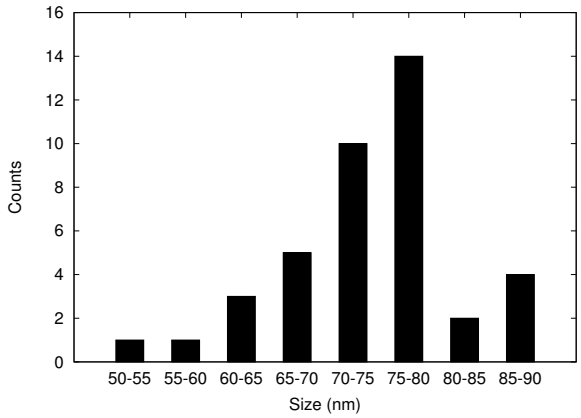

FIG. 6. Distribution of the cubes' sizes for a sample of 40 cubes.

The size distribution of the cubes can be estimated from the SEM images. Figure6 shows the statistical distribution of the different sizes. Since different sizes lead

to different resonance frequencies, a surface covered with cubes of different sizes leads to an broadening and a reduction in the depth of the reflectance spectrum.

The size dispersion can be taken into account by considering that the absorption by the surface is a statistical average of the absorption by cubes with different sizes. Full 3D simulations have been made using a Fourier Modal Method for several cube sizes, and the absorption a_w for each size w and for a concentration of c_0 has been computed using

$$a_w(\lambda) = r_0(\lambda) - r_w(\lambda), \tag{8}$$

where r_w is the reflection coefficient of a surface covered by cubes with a size w and r_0 is the reflection coefficient of the bare gold film. The main assumption we make here is that the absorption for a given size is directly proportional to the surface coverage (i.e. that the cubes have a well defined cross-section). Simulations indicate that this assumption is perfectly valid, but only for a low enough concentration: for high concentrations, simulations show that the absorption saturates and is no longer dependent on the period. As long as the assumption of a well defined cross-section for each cube can be considered valid, the reflectance for a concentration c can be written

$$r(\lambda) \simeq r_0(\lambda) + \int \frac{c}{c_0\sqrt{2\pi\sigma^2}}\, e^{-\frac{(w-\bar{w})}{2\sigma^2}}\, r_w(\lambda)\, \mathrm{d}w. \tag{9}$$

if a gaussian distribution (with an average of $\bar{w} = 62$ nm and a standard deviation of $\sigma = 10$ nm here) has been assumed for the sizes.

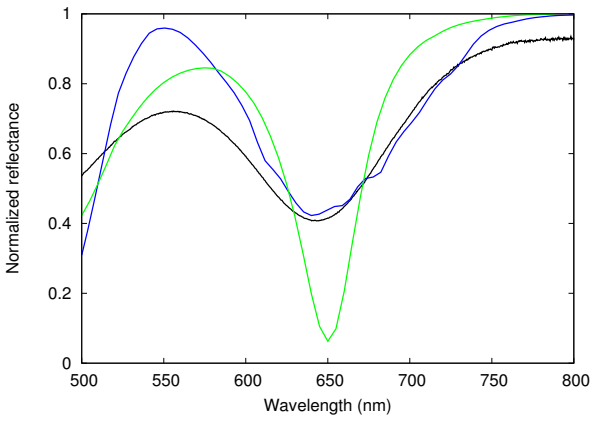

FIG. 7. Comparison between the experimental data in normal incidence for a 7.3% concentration of the nanocubes(black curve), a simulation for a 4.3% surface coverage by a perfectly uniform population of 62 nm cubes (green curve) and the model of the reflectance taking into account the size dispersion for a 7.3% concentration (blue curve).

The large distribution of the nanocubes size erodes the quality of the absorption from the cube covered surface. Figure 7 shows that the reflectance for a 7.3% surface coverage of the nanocubes which were fabricated is accurately predicted by the model when the actual size distribution is taken into consideration. It would clearly be desirable to utilize the most uniform population of nanocubes that can be prepared, as this would improve the response at a select frequency. The model is accurate for predicting the dip of the reflectance that can be directly attributed to the resonance of the nanoantennas. However, a part of the light is actually scattered or absorbed by different phenomena (excitation of surface waves for instance, interaction between particles), and this is not perfectly reproduced by the model because these phenomena have much less impact for the low concentrations that were used to estimated the efficiency of the absorption.

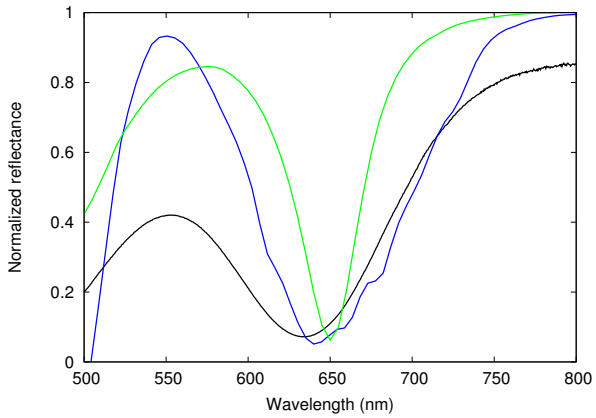

FIG. 8. Comparison between the experimental data in normal incidence for a 17.1% surface coverage of the nanocubes which we fabricated(black curve), a simulation for a 4.3% surface coverage by perfectly uniform 62 nm cubes (green curve) and the model of the reflectance taking into account the size dispersion for a 12% surface coverage (blue curve).

In an attempt to reach complete absorption, using the cubes which were available experimentally, we increased the surface coverage of our sample to 17%. While near perfect absorption can theoretically be achieved with a much lower concentration of uniformly sized cubes, according to our model a 12% concentration of cubes with a size distribution approximating our fabricated cubes would produce a reflectance close the measured reflectance of the 17% coverage sample, as shown figure 8.

Definition of effective absorption cross-section

An important figure of merit for quantifying the absorbance of the nanocube surface is that of effective absorption efficiency. The association of either scattering or absorption cross-sections to individual nanocubes is complicated by the ambiguity in the effective incident

field, which includes the actual incident plane wave plus reflected fields. Thus, we define the effective absorption cross-section as the absorbed power divided by the intensity of the incident plane wave, which provides a practical measure. Note that this absorption cross-section is only relevant to the configuration considered; the absorption cross-section for a cube in free space would be quite different. We further define the effective absorption efficiency as the effective absorption cross-section divided by the physical cross-sectional area of the cube.